Synthesis of Acid Hydrolysis Lignin-g-Poly-(Acrylic Acid) Hydrogel Superabsorbent Composites and Adsorption of Lead Ions

Yajie Sun,[a] Yanli Ma,[a,*] Guizhen Fang,[a] Shujun Li,[a] and Yujie Fu [b]

A series of acid hydrolysis lignin-g-poly-(acrylic acid) (AHL-g-PAA) composites was prepared by grafting acid hydrolysis lignin on the surface of the polyacrylic acid network. The results of structure analysis revealed that AHL-g-PAA had been grafted. The surface morphologies of the hydrogels were improved, as shown by scanning electron microscopy observation. The AHL-g-PAA hydrogel had high water absorption and it possessed sensitivity to external pH stimulus. This study also revealed that the adsorption capacity of AHL-g-PAA was 235 mg/g for Pb(II) ions. The adsorption kinetics data could be described by the pseudo-second-order model, and the adsorption isotherm agrees well with the Langmuir model.

Keywords: Acid hydrolysis lignin; Lead adsorption; Polyacrylic acid; Biodegradable materials; Gels; Grafting; Copolymers; Crosslinking

Contact information: a: Material Science and Engineering College, Northeast Forestry University, Harbin, 150040, P.R. China; b: Postdoctoral Research Station of Biological Station, Northeast Forestry University, Harbin,150040, China;
**Corresponding author: myl219@sohu.com*

INTRODUCTION

Composite hydrogels are crosslinked three-dimensional network structures of hydrophilic homopolymers or copolymers (Liu *et al*. 2013). They can swell easily in aqueous solution and have high water absorbing capacity. Hydrogels are used as effective adsorbents for various applications, including agriculture, biomedicine, as antibacterial materials, tissue engineering, drug delivery, separation of heavy metal ions (Guilherme *et al*. 2007; Murthy *et al*. 2008), and dye molecules from water. Usually, hydrogels are prepared from synthetic polymers by radical-induced copolymerization, frontal copolymerization, graft copolymerization, cross-linking, and ionizing radiation materials (Marandi *et al*. 2008). Compared with other adsorbents, composite hydrogels possess many functional groups and a unique network structure, and they can absorb and trap metal ions or ionic dyes from effluents more efficiently (Yetimoğlu *et al*. 2007). However, most hydrogels cannot be used extensively for various applications because of their low stability, high production costs, and latent toxicity (Shang *et al*. 2008). These drawbacks can be overcome by the addition of naturally available raw materials, which are low-cost, renewable, non-toxic, and biodegradable (Wang *et al*. 2008). The naturally available raw materials contain or can be prepared with functional groups such as carboxylic acid, amine, hydroxyl, amidoxime, and sulfonic acid groups. These groups, when attached to polymeric networks, can be tailored easily for specific applications. Starch, cellulose, chitosan, and guar gum have been utilized to fabricate various multi-component superabsorbents, and

some encouraging hybrid performances have been achieved (Wang and Wang 2009; Chang *et al*. 2010).

Lignin is a renewable amorphous biopolymer consisting of phenylpropane units linked through various ether and carbon-carbon bonds and is one of the most abundant biopolymers on earth. Lignin is the only natural source of aromatic functionality in wood, and it can be utilized effectively for various applications. The study of modified hydrogels using lignin has made great progress. There have been some studies of the preparation of hydrogels using lignin (Luo *et al.* 2015). The cross-linking of milled wood lignin and kraft lignin with epichlorohydrin is a promising work concerning lignin-based hydrogels (El-Zawawy 2005). Thus, the potential range of application of lignin-based gels has been broadened considerably. Studies of the adsorption of base metals using various types of lignin have also been reported (Ludvik and Zuman 2000). Crosslinked lignocatechol exhibited excellent adsorption characteristics for the metal ions tested, especially for Pb(II) ions (Uraki *et al*. 2006). With superior efficiency, its preparation method is very simple and the production cost is cheap. Hence, this novel lignin-based adsorption gel is suitable for repeated use and may be an efficient adsorbent for environmental remediation.

With this in mind, in the present study, a composite hydrogel was prepared with lignin and an acrylic copolymer, based on previous work done to determine the optimal conditions for preparation of acid polymerization and acid hydrolysis lignin (Ma *et al*. 2012). Therefore, in this study, the best dosage of acid hydrolysis lignin was considered. Hydrogels were characterized by swelling characteristics, network parameters, solid state nuclear magnetic resonance spectroscopy (SSNMR), scanning electron microscopy (SEM), Fourier transform infrared (FTIR), and wide angle X-ray diffraction (XRD). Hydrogel composites were prepared and used as adsorbents for Pb(II) ion adsorption. The adsorption kinetics and isotherms of the composites toward Pb(II) ions were studied, and the adsorption mechanism was also discussed.

EXPERIMENTAL

Materials

Commercial lignin was supplied by Tralin Paper Co., Ltd., (Shandong, China). Lignin was isolated by alkali-assisted extraction from wheat straw, to give a composition containing 82.69% lignin, 8.35% carbohydrates, and 8.96% ash. The total hydroxyl content of the lignin was found to be 2.95 mmol g^{-1}. All reagents were of analytical grade and were used without further purification. Acrylic acid (AA), ammonium persulfate (APS), and *N*, *N*′-methylenebisacrylamide (MBA) were obtained from the Aladdin Chemistry Co., Ltd., (Guangzhou, China). Sodium hydroxide (NaOH), ferrous sulfate ($FeSO_4$), anhydrous ethanol (EtOH), and hydrogen peroxide (H_2O_2, 30%) were purchased from Shanghai Reagent Corp. (Shanghai, China). Deionized water with a pH value of approximately 6.9 was used throughout the study.

Methods

Preparation of acid hydrolysis lignin

The pH of the lignin fluid was adjusted to a value of 2 using 1 M hydrochloric acid, the solution was heated to 80 °C for 4 h, and the filter cake was washed to neutral pH using a suction filter. The acid hydrolysis lignin was then dried to constant weight at 50 °C. The dry lignin sample was powdered until samples of lower than 120-mesh sizes were obtained.

Preparation of AHL-g-PAA hydrogel

A solution of the acid hydrolysis lignin was prepared by the addition of the lignin powder (1 g) to a solution of NaOH (1.25 M). The resulting solution was heated to 60 °C with stirring and purged with N_2 for 30 min. Ferrous sulfate (0.05 g) and H_2O_2 (1 mL) were then added, and the mixture was held at 60 °C for 0.5 h under N_2 to allow the generation of free radicals. After this time, the reaction mixture was cooled to 40 °C, and a mixture of AA (monomer, 1.56 mL, neutralization degree 60%), MBA (cross-linker, 0.7 wt.%), and APS (initiator, 1 wt.%) were added to the flask. The temperature was then increased to 60 °C, and this temperature was maintained for 2 h under N_2 to complete the polymerization process. After cooling to 20 °C and allowing the crude mixture to stand for 4 h, AHL-g-PAA hydrogels were obtained. The resulting product was then washed with 30 mL of anhydrous ethanol three times and extracted with acetone at 20 °C for 24 h to dissolve the homopolymer and lignin. The hydrogel was then dried to constant weight at 70 °C. Dry AHL-g-PAA was then ground in a circular cylinder (5-mm diameter, 2-mm thickness) using a gel puncher (Tiancheng, Shanghai, China). This method was used to prepare materials with polymers and acid hydrolysis lignin in various mass ratios. The control sample (PAA) was also prepared according to the above procedure without the addition of the acid hydrolysis lignin.

Characterization

Solid state nuclear magnetic resonance spectroscopy (^{13}C MAS NMR) analysis for the macro-molecular structure characterizations of acid hydrolysis lignin and AHL-g-PAA copolymers were recorded under ambient temperature on a Bruker Advance 300 MHz spectrometer (Bruker, Germany). The morphology of AHL-g-PAA was studied using scanning electron microscopy (SEM) (FEI Quanta 200, FEI Ltd., USA). Fourier transform infrared (FTIR) studies were performed using a Magna-IR560 spectrometer (Thermo Nicolet Corporation, USA).

Swelling studies

Gravimetric methods were used to measure the swelling behaviors of the hydrogel samples. A sample of each hydrogel (0.10 g) was immersed in deionized water (100 mL) at 20 °C for 24 h to reach swelling equilibrium. The swollen samples were then filtered through 100-mesh gauze and weighed. The equilibrium water absorbency was calculated according to Eq. 1,

$$Q_{eq} = (M - M_0)/M_0 \quad (1)$$

where Q_{eq} (g/g) is the water absorbency calculated per gram of dried sample. M_0 (g) and M (g) are the weights of the dry and swollen samples, respectively. All assays were carried out in triplicate, and the average was used in the analysis.

Adsorption

Adsorption experiments were carried out by agitating 0.1 g of hydrogel with 100 mL of a 350 mg/L Pb(II) ion solution (pH=5.5) in a shaker at 30 °C/120 rpm. At intervals, 5-mL aliquots were sampled and analyzed for residual Pb(II) concentration until the adsorption equilibrium was achieved. The Pb(II) content was analyzed by TAS-990 atomic absorption spectrometry (Persee, Beijing, China). The adsorption capacity of the hydrogel for Pb(II) ions was calculated using the following equation,

$$q = (C_0 - C_e)V/m \quad (2)$$

where q is the amount of Pb(II) adsorbed at time t (min) or at equilibrium (mg/g), C_0 and C_e are the initial and final concentration of Pb(II) (mg/L), respectively, V is the volume of Pb(II) solution used (L), and m is the mass of the hydrogel used (g).

RESULTS AND DISCUSSION

Composite Morphology

Scanning electron micrographs and swelling equilibrium images of PAA and AHL-g-PAA hydrogels are shown in Fig. 1. The water absorption properties of hydrogels and adsorption performance are related to its surface properties and its network structure. Contrast SEM pictures of PAA (Fig. 1a) and AHL-g-PAA (Fig. 1c) indicate that acid hydrolysis lignin had an obvious influence on the network structure of PAA. From Fig. 1a, it can be seen that the network structure of PAA was like a closed honeycomb cell. With the addition of lignin, this network structure was gradually replaced with a porous structure with a noticeably rougher surface morphology, which leads to increased surface area (Fig. 1c).

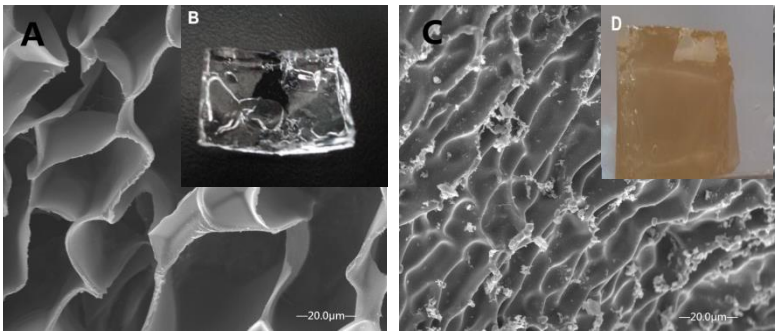

Fig. 1. Scanning electron micrographs of (a) PAA, (c) AHL-g-PAA; the swelling equilibrium images of (b) PAA, (d) AHL-g-PAA

Synthesis of AHL-g-PAA Graft Copolymer

Figure 2a is the ^{13}C MAS NMR results for acid hydrolysis lignin and AHL-g-PAA, which shows that the AHL-g-PAA spectrum mostly contained carboxyl groups (from δ 185 to 175 ppm) and saturated aliphatic carbon chains (from δ 50 to 15 ppm). Characterization of acid hydrolysis lignin was very obvious in the ^{13}C MAS NMR. As shown, the characteristic peaks corresponded to the basic aromatic ring (C=C from δ 140 to 110 ppm) and aromatic ring with branched chain of C-C bonds (from δ 75 to 10 ppm). The NMR spectra of AHL-g-PAA also showed a characteristic peak from δ 185 to 170 ppm caused by the effect of carboxylic acid.

The characterization of hydrogel using FTIR analysis was performed to study the interaction between the acid hydrolysis lignin and the PAA hydrogel. The FTIR results of acid hydrolysis lignin, PAA, and AHL-g-PAA are shown in Fig. 2b. New peaks appeared in the AHL-g-PAA spectrum at 1326 cm^{-1} (the in-plane bending vibration of –OH group), 1114 and 1220 cm^{-1} (C-O stretching vibration band), and 894 cm^{-1} (the symmetric stretching vibration of C-O-C) coming from acid hydrolysis lignin. These absorption bands also appeared in the spectra of AHL-g-PAA, which provided strong evidence of grafting

and confirmed that AHL-g-PAA hydrogel composites were formed. In addition, the increase in the peak height at 1714 cm^{-1} is also evidence for the hydrogel formation.

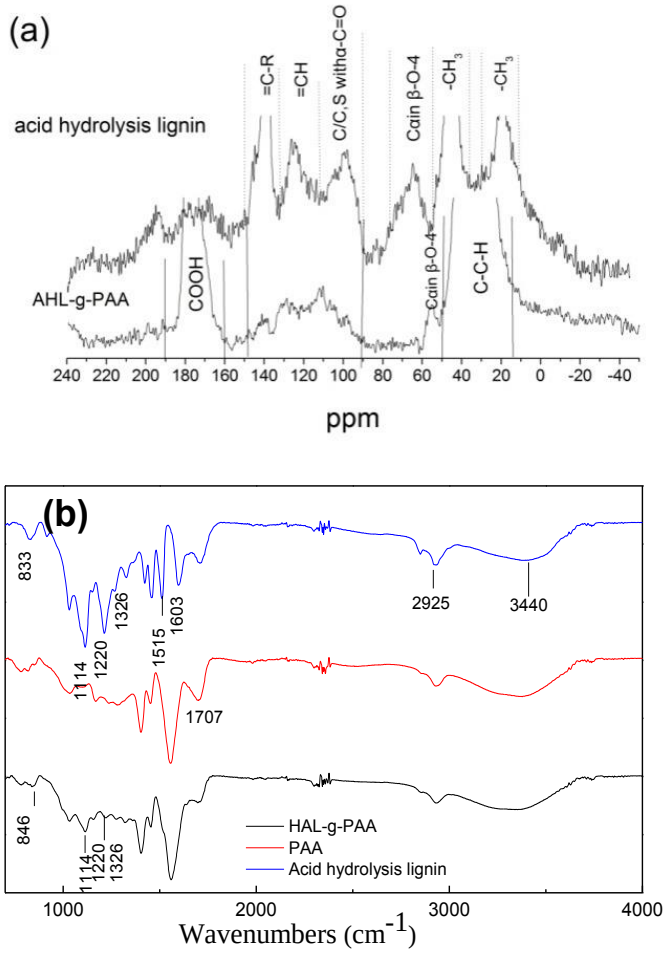

Fig. 2. (a) The ^{13}C MAS NMR of acid hydrolysis lignin and AHL-g-PAA; (b) FTIR spectra of acid hydrolysis lignin, PAA, AHL-g-PAA

Swelling Sensitivity of the Hydrogels

Figure 3a shows the water uptake of PAA and AHL-g-PAA in distilled water. It can be seen that, after polyacrylic acid had reacted with the acid hydrolysis lignin, the swelling ratio increased noticeably, from 180 to 392 g/g. The reason for the higher water absorption value can be attributed to the change in porosity and surface morphology resulting from the composite AHL-g-PAA formed from the acid hydrolysis lignin. Acid hydrolysis lignin graft polyacrylic acid has the advantage of contraction speed because of the loose structure and possesses low density. Compared with PAA, AHL-g-PAA holds high efficiency of water loss.

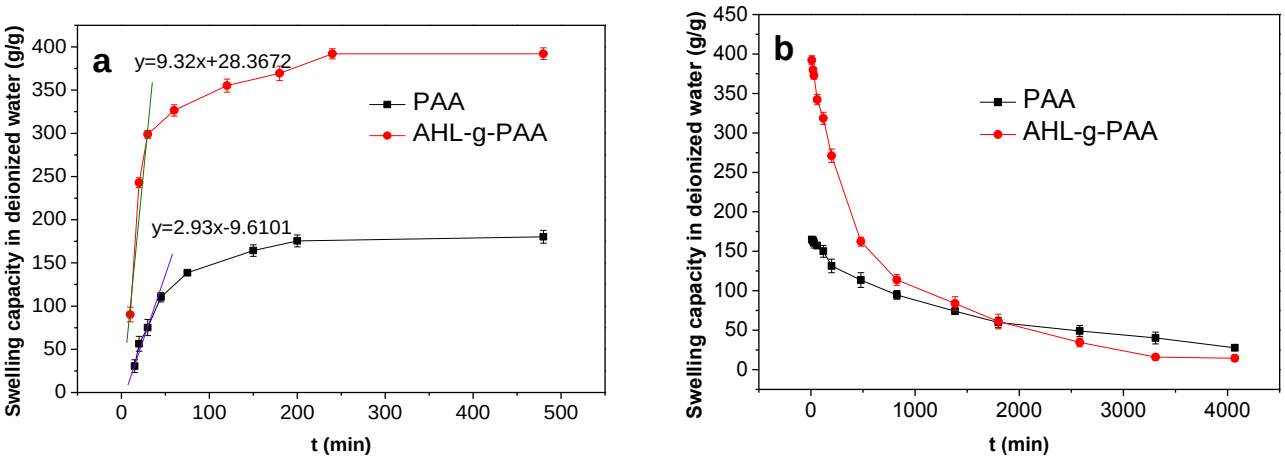

Fig. 3. PAA and AHL-g-PAA: (a) swelling capacity in deionized water; (b) deswelling capacity

The microstructure of porous characteristics can speed up the adsorption of water molecules. Also it has an effect on the curve of the expansion rate of the gel. Porous structure reduces the internal diffusion resistance when water molecules enter in gel and change the distribution of internal diffusion resistance gel, and this will change curve of the form to a certain extent. So, at the beginning of the adsorption, the swelling rate of AHL-g-PAA was greater than the swelling rate of PAA. The AHL-g-PAA composite released water (from 0 to 500 min) rapidly, and a higher ability to lose water was observed, except for AHL-g-PAA (in Fig. 3b). This was attributed to the new network structure of AHL-g-PAA, which was suitable for the in and out movement of the water molecules within the network.

Effects of Contact Time for Pb(II)

The effects of contact time on the adsorption capacities of PAA and AHL-g-PAA were studied, as shown in Fig. 4. The adsorption capacity of AHL-g-PAA was found to be 244.12 mg/g, while the control sample without acid hydrolysis lignin showed an adsorption capacity of 104 mg/g for Pb(II) ion adsorption. The change in adsorption capacity may be ascribed to the following reasons. First, the carboxyl groups are the main functional groups responsible for adsorption of Pb(II) ions. In the adsorption process of hydrogels composites for Pb(II) ions, the addition of lignin improves the gel network structure by damaging parts of the network structure of polyacrylic acid, which leads to reduction in crosslinking intensity, reduced number of carboxyl groups, and increased activated points (Jing *et al*. 2009). At the same time, the new structure formed benefits the absorption capacity through the network structure of polyacrylic acid.

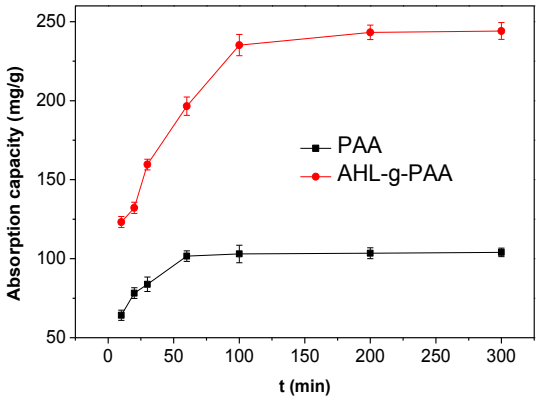

Fig. 4. Effect of contact time on adsorption of Pb(II)

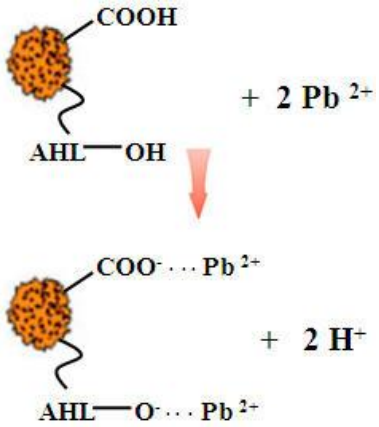

Fig. 5. Mechanism of adsorption of Pb (II) on AHL-g-PAA

Adsorption Kinetics for Pb(II)

The controlling mechanism of adsorption process depends on the physical and chemical properties of adsorbent and various other adsorption conditions. To examine the controlling mechanism of adsorption processes such as mass transfer and chemical reaction, the pseudo-first-order and pseudo-second-order equations (Zhang and Wang 2010) were used to test the experimental data,

$$\log(q_{1e}-q_t) = \log q_{1e} - k_1 t /2.303 \quad (3)$$

$$t/ q_t = 1/(k_2 q_{2e}^2) + t /q_{2e} \quad (4)$$

where q_{1e}, q_{2e}, and q_t (mg/g) represents the amount of lead ions adsorbed per unit mass of adsorbent at equilibrium and at any time t, respectively. The parameters k_1 (min^{-1}) and k_2 (g/ (mg min)) are the rate constants of the pseudo-first-order and pseudo-second-order models, respectively. From the slope and intercept of the plot of $\log(q_{1e}-q_t)$ *vs.* t, k_1, and q_{1e} can be obtained, and in the same way, q_{2e} and k_2 can be obtained from the plot of t/q_t against t.

The experimental data were analyzed by the two kinetic models, and the parameters calculated from above equations and correlation coefficients are listed in Table 1. The coefficients of determination R^2 for the pseudo-second-order kinetic plots for all the hydrogels studied were above 0.99, indicating that the pseudo-second-order kinetic model can well describe the experimental data. The calculated q_{1e} did not show reasonable values, which suggested the pseudo-first-order model did not fit the adsorption process and confirmed the fit of the pseudo-second-order model for the adsorption system, validating the viewpoint mentioned above. The results suggested that the pseudo-second-order adsorption mechanism dominated the adsorption process.

Table 1. The Pseudo-First-Order and Pseudo-Second-Order Model Parameters for Pb(II) Ions Adsorbed onto Adsorbents

Samples	Q_m	Pseudo-first-order model			Pseudo-second-order model		
		q_{1e}	k	R^2	q_{2e}	k	R^2
PAA	104.4421	131.419	0.0085	0.9129	110.011	0.88×10^3	0.9976
AHL-g-PAA	245.0014	272.415	0.0033	0.9735	242.718	3.41×10^4	0.9979

Adsorption Isotherms for Pb(II) Ions

It is important to establish suitable correlations for the adsorption equilibrium data using isotherm equations, which can help to understand the adsorption process and design the adsorption process. Many isotherm models have been proposed to explain the adsorption equilibrium, and the most commonly used isotherm models for liquid–solid adsorption are Langmuir and Freundlich (Zhang *et al*. 2012) models. The equilibrium data obtained were tested with respect to the two isotherm models,

$$\text{Langmuir equation:}\quad C_e/q_e = C_e/q_m + 1/bq_m \tag{5}$$

where q_m (mg/g) represents the maximal adsorption capacity to form a monolayer in the system; q_e (mg/g) represents the amount of solute adsorbed per unit weight of the adsorbent at equilibrium; C_e (mg/L) is the equilibrium solute concentration in solution, and b (L/mg) is the Langmuir constant. The plot of C_e/q_e against C_e would be a straight line, and then q_m and b can be obtained from the slope and intercept of the plot.

The essential feature of the Langmuir isotherm is R_L (Yan *et al*. 2012), which is a dimensionless separation factor or equilibrium parameter, defined as,

$$R_L = 1/(1 + bC_i) \tag{6}$$

where b and C_i are the same as defined above. The value of R_L is an indicator of the shape of adsorption isotherm to be favorable or unfavorable. The value of R_L between 0 and 1 indicates a favorable adsorption, while R_L suggests unfavorable adsorption and the adsorption process is linear adsorption if R_L=1, while R_L=0 represents irreversible adsorption.

$$\text{Freundlich equation: } \ln q_e = \ln k_f + (\ln C_e)/n \tag{7}$$

In Eq. 7, k_f (L/mg) and $1/n$ are Freundlich constants, related to adsorption capacity and adsorption intensity, respectively, and the other symbols are the same as defined above. If value of $1/n$ is in the range of 0 to 1, the adsorption process is feasible and favorable. From the slope and intercept of the plot of $\ln q_e$ *vs.* $\ln C_e$, $1/n$ and k_f can be obtained, respectively.

The constant parameters and correlation coefficients were calculated from the Langmuir and Freundlich models, as summarized in Table 2. It can be seen that the values of coefficients of determination for the Langmuir equation were higher than the other two isotherm values, which indicated the Langmuir isotherm correctly fitted the equilibrium data, confirming the monolayer coverage of Pb(II) ions onto the hydrogel composites. It was obvious that the values of R_L in the range of 0.03 to 0.53 confirmed the favorable uptake of the adsorption process. Meanwhile, the lower R_L values at higher initial Pb(II) ion concentrations suggested that the adsorption was more favorable at higher concentrations, consistent with the results obtained from the effect of initial concentration.

On the other hand, Table 3 presents the comparison of biosorption capacity (mg/g) of AHL-g-PAA for Pb(II) ions with that of other biosorbents reported in literature. The biosorption capacity of AHL-g-PAA for Pb(II) was higher than that of the majority of other biosorbents mentioned. Therefore, it can be noteworthy that the AHL-g-PAA has important potential for the removal of Pb(II) ions from aqueous solution.

Table 2. Estimated Adsorption Isotherm Parameters for Pb(II) Adsorption

Samples	Langmuir model				Freundlich model		
	q_m	b	R^2	R_L	k_f	$1/n$	R^2
PAA	105.7444	0.08728	0.984	0.07-0.53	0.0271	0.1078	0.9051
AHL-g-PAA	259.8875	0.0999	0.9818	0.03-0.27	0.0351	0.1698	0.9342

Table 3. Comparison of Biosorption Capacity (mg/g) for Pb(II) On Different Biosorbents in the Literature

Biosorbent	Pb(II)	pH	References
AHL-g-PAA	244.12	5.5	Present study
Saw dust	21.05	-	Li 2007
Modified peanut husk	29.14	-	Li 2007
Expanded perlite(EP)	13.39	5	Sari *et al.* 2007
Ulva lactuca	34.7	5	Sari *et al.* 2008
Lactarius scrobiculatus	56.2	5.5	Anayurt *et al.* 2009
Pseudomonas putiada	32.6	5.5	Uslu and Tanyol 2006
Parmelina tiliaceae	75.8	5	Uluozlu *et al.* 2008

Mechanism of Adsorption for Pb(II)

The mechanism of any adsorption process is an important component to understand the process as well as to know the characteristics of the material that help to design a new adsorbent for the future applications. Electrostatic interactions between the positively charged Pb(II) and the negative charge on AHL-g-PAA can give rise to ion exchange (Eq. 9). The positively charged Pb (II) ions are adsorbed onto the AHL-g-PAA surface *via* chemical ion exchange or electrostatic attraction, as suggested in Fig. 5.

$$(\text{OH-AHL-g-PAA-COOH}) + 2Pb^{2+} \longrightarrow \quad Pb^{2+}(^{-}\text{O-AHL-g-PAA-COO}^{-})Pb^{2+} + 2H^{+} \quad (8)$$

CONCLUSIONS

1. A polyacrylic acid lignin hydrogel (AHL-g-PAA) was prepared by grafting acid hydrolysis lignin with polyacrylic acid. After forming AHL-g-PAA, the surface morphologies, swelling capabilities, and adsorption capacities were greatly improved.
2. The maximum water absorbency under optimum conditions for superabsorbent hydrogel composite was 392 g/g in distilled water, and the adsorption capacity was found to be 244.12 mg/g for Pb(II) ions.
3. The adsorption kinetics data could be described by the pseudo-second-order model, and

the adsorption isotherm agreed well with the Langmuir model.

4. This low-cost and environmentally friendly production has considerable potential for water absorption and are promising adsorbents for Pb(II) ions from aqueous solution.

ACKNOWLEDGMENTS

The authors are grateful for support by the Fundamental Research funds for the Central Universities (No. DL13CB09), the Youth Science Foundation of Heilongjiang Province of China (No. QC2014C011), and the Chinese "Twelfth Five Year" National Science and Technology Plan Project in Rural Areas (No. 2012BAD24B0403).

REFERENCES CITED

Anayurt, R. A., Sari, A., and Tuzen, M. (2009). "Equilibrium, thermodynamic and kinetic studies on biosorption of Pb(II) and Cd(II) from aqueous solution by macrofungus (*Lactarius scrobiculatus*) biomass," *Chem. Engin. J.* 151(1–3), 255-261. DOI:10.1016/j.cej.2009.03.002

Chang, C., Duan, B., Cai, J., and Zhang, L. (2010). "Superabsorbent hydrogels based on cellulose for smart swelling and controllable delivery," *Eur. Polym. J.* 46(1), 92-100. DOI: 10.1016/j.e Lellis. urpolymj.2009.04.033

El-Zawawy, W. K. (2005). "Preparation of hydrogel from green polymer," *Polym. Adv. Technol.* 16(1), 48-54. DOI: 10.1002/pat.537

Guilherme, M. R., Reis, A. V., Paulino, A. T., Fajardo, A. R., and Muniz, E. C., and Tambourgi, E. B. (2007). "Superabsorbent hydrogel based on modified polysaccharide for removal of Pb^{2+} and Cu^{2+} from water with excellent performance," *J. Appl. Polym. Sci.* 105(5), 2903-2909. DOI: 10.1002/app.26287

Jing, X. S., Liu, F. Q., Xin, Y., Ling, P. P., Li, L. J., and Chao, L. (2009). "Adsorption performances and mechanisms of the newly synthesized N,N′-di (carboxymethyl) dithiocarbamate chelating resin toward divalent heavy metal ions from aqueous media," *J. Hazard. Mater.* 167(1-3), 589-96. DOI:10.1016/j.jhazmat.2009.01.020

Liu, J., Su, Y., Li, Q., Yue, Q. Y., and Gao, B. Y. (2013). "Preparation of wheat straw based superabsorbent resins and their applications as adsorbents for ammonium and phosphate removal," *Bioresour. Technol.* 143(C), 32-39. DOI: 10.1016/j.biortech.2013.05.100

Ludvik, J., and Zuman, P. (2000). "Adsorption of 1,2,4-triazine pesticides metamitron and metribuzin on lignin," *Microchem. J.* 64(1), 15-20. DOI: 10.1016/S0026-265X(99)00015-6

Luo, H. C., Ren, S. X., Ma, Y. L., Fang, G. Z., and Jiang, G. Q. (2015). "Preparation and properties of kraft lignin-N-isopropyl acrylamide hydrogel," *BioResources* 10(2), 3507-3519. DOI: 10.15376/biores.10.2.3507-3519

Ma, Y. L., Wang, R. R., and Fang, G. Z. (2012). "Preparation and release performance of polyacrylic acid grafted alkali lignin-based iron fertilizer," *Trans. Chin. Soc. Agric. Eng.* 28(18), 208-214. DOI: 10.3969/j.issn.1002-6819.2012.18.030

Marandi, G. B., Esfandiari, K., Biranvand, F., Babapour, M., Sadeh, S., and Mahdavinia, G. R. (2008). "pH sensitivity and swelling behavior of partially hydrolyzed formaldehyde-crosslinked poly(acrylamide) superabsorbent hydrogels," *J. Appl. Polym. Sci.* 109(2), 1083-1092. DOI: 10.1002/app.28205

Murthy, P. S. K., Mohan, Y. M., Varaprasad, K., Sreedhar, B., and Raju, K. M. (2008). "First successful design of semi-IPN hydrogel-silver nanocomposites: A facile approach for antibacterial application," *J. Colloid. Interface. Sci.* 318(2), 217-224. DOI:10.1016/j.jcis.2007.10.014

Sarı, A., and Tuzen, M. (2008). "Biosorption of Pb(II) and Cd(II) from aqueous solution using green alga (*Ulva lactuca*) biomass," *J. Hazard. Mater.* 152(1), 302-308. DOI:10.1016/j.jhazmat.2007.06.097

Sarı, A., Tuzen, M., Cıtak, D., and Soylak, M. (2007). "Adsorption characteristics of Cu(II) and Pb(II) onto expanded perlite from aqueous solution," *J. Hazard. Mater.* 148(1-2), 387-94. DOI:10.1016/j.jhazmat.2007.02.052

Shang, J., Shao, Z., and Chen, X. (2008). "Chitosan-based electroactive hydrogel," *Polymer* 49(25), 5520-5525. DOI: 10.1016/j.polymer.2008.09.067

Uluozlu, O., Sari, A., Tuzen, M., and Soylak, M. (2008). "Biosorption of Pb(II) and Cr(III) from aqueous solution by lichen (*Parmelina tiliaceae*) biomass," *Bioresour. Technol.* 99(8), 2972-2980. DOI:10.1016/j.biortech.2007.06.052

Uraki, Y., Imura, T., Kishimoto, T., and Ubukata, M. (2006). "Body temperature-responsive gels derived from hydroxypropylcellulose bearing lignin. II: Adsorption and release behavior," *Cellulose* 13(2), 225-234. DOI:10.1016/j.carbpol.2004.05.019

Uslu, G., and Tanyol, M. (2006). "Equilibrium and thermodynamic parameters of single and binary mixture biosorption of lead (II) and copper (II) ions onto *Pseudomonas putida*: Effect of temperature," *J. Hazard. Mater.* 135(1–3), 87-93. DOI:10.1016/j.jhazmat.2005.11.029

Wang, C., Liu, H., Gao, Q., Liu, X., and Tong, Z. (2008). "Alginate-calcium carbonate porous microparticle hybrid hydrogels with versatile drug loading capabilities and variable mechanical strengths," *Carbohydr. Polym.* 71(3),476-480. DOI: 10.1016/j.carbpol.2007.06.018

Wang, W. B., and Wang, A. Q. (2009). "Preparation, characterization and properties of superabsorbent nanocomposites based on natural guar gum and modified rectorite," *Carbohydr. Polym.* 77(3), 891-897. DOI: 10.1016/j.carbpol.2009.03.012

Yan, H., Yang, L., Yang, Z., Yang, H., Li, A., and Cheng, R. (2012). "Preparation of chitosan/poly(acrylic acid) magnetic composite microspheres and applications in the removal of copper(II) ions from aqueous solutions," *J. Hazard. Mater.* 229-230, 371-380. DOI: 10.1016/j.jhazmat.2012.06.014

Yetimoğlu, E. K., Kahraman, M. V., Ercan, Ö., Akdemir, Z. S., and Apohan, N. K. (2007). "N-vinylpyrrolidone/acrylic acid/2-acrylamido-2-methylpropane sulfonic acid based hydrogels: Synthesis, characterization and their application in the removal of heavy metals," *React. Funct. Polym.* 67(5), 451-460. DOI: 10.1016/j.reactfunctpolym.2007.02.007

Zhang, J. P., and Wang, A. Q. (2010). "Adsorption of Pb(II) from aqueous solution by chitosan-*g*-poly(acrylic acid)/ attapulgite/sodium humate composite hydrogels," *J. Chem. Eng. Data.* 55(7), 2379-2384. DOI: 10.1021/je900813z

Zhang, P. Y., Zhang, G. M., Dong, J. H., Fan, M. H., and Zeng, G. M. (2012). "Bisphenol A oxidative removal by ferrate (Fe(VI)) under a weak acidic condition," *Sep. Purif. Technol.* 84(9), 46-51. DOI:10.1016/j.seppur.2011.06.022

Article submitted: July 21, 2015; Peer review completed: September 27, 2015; Revised version received: April 25, 2016; Accepted: April 26, 2016; Published: May 9, 2016.
DOI: 10.15376/biores.11.3.5731-5742